European Academy of Applied and Social Sciences – www.euraass.com

European Journal of Climate Change

https://www.euraass.com/ejcc/ejcc.html

Research Article

Geography and Demographics of Extreme Urban Heat Events in Santa Clara County, California

Christopher Potter

CASA Systems 2100, LLC, Los Gatos, CA 95020 USA.

Abstract

Summer heat waves in Northern California continue to break records for extreme temperatures and put vulnerable urban populations at increasing risk for adverse health impacts. An analysis of Landsat land surface temperature data was conducted in this study to better understand the geography and demographics of extreme urban heat events in Santa Clara County and the city of San Jose, California. The influence of several urban cover features including streets/roadways, parcel sizes and densities, impervious surfaces, and irrigated shrub/lawn cover were determined for county-wide surface heat patterns in early August 2020. Results showed that the surface temperature of the largest impervious (high-asphalt) surface features was significantly higher, at a mean value of 45 °C, than the majority of the other areas across the entire county. In contrast, urban tracts with even partial coverage by irrigated green lawns, shrubs, and small trees had notable cooling effects on summer surface temperatures. Social demographic and household population variables from the U. S. Census Bureau were correlated against satellite surface temperature by census tract to reveal significant associations of family structure and education levels with local neighbourhood heat conditions.

Keywords: Urban heat, Landsat, Santa Clara County, San Jose, California, impervious surfaces.

1. Introduction

Among all weather-related hazards, extreme urban heat events have become the leading cause of fatalities in United States over the past several decades (Borden and Cutter, 2008; Wong et al., 2013, Hoffman et al., 2019). Temperature extremes can exacerbate poor health conditions, particularly for persons that have been previously compromised by cardiovascular and respiratory illness, leading to an increase in heat-related mortality (CDC, 2006). Moreover, Habeed et al. (2015) reported that from 1960 to 2010, the length of heat waves is increasing by a fifth of a day (on average) in major U. S. cities, and the length of the heat wave season (time between first and last heat wave) has been increasing by six days per decade.

Extreme heat events or heat "waves" have been defined in various ways in previous studies. Habeed et al. (2015) characterized such an event as a minimum temperature exceedance of the local 85th percentile threshold that occurs for two or more consecutive

days. For the western U. S. region, Guirguis et al. (2011) defined a heat wave according to daily temperatures (minimum and maximum) exceeding the 95th percentile thresholds computed from local daily climatologies over the May through September warm season. For health-related applications, practitioners tend to stress duration and focus on events that last at least two days. Nonetheless, public heat warnings may be issued when maximum air temperature is forecast to exceed 35 °C on any one day, or above 25 °C for at least five days of which at least three days threaten temperatures above 30 °C (Gershunov et al., 2009).

In California, heat waves can occur as two general types: dry daytime events and humid night time events (Gershunov, and Guirguis, 2012). The peak of the heat wave season in California typically occurs at the seasonal temperature peak from late July to early August for all inland regions. However, because of the complex topography and many localized microclimates, regional-scale heat waves in Northern California can be expressed differently from coastal zones to inland valleys. Gershunov and Guirguis (2012) reported that before about 1995, dry daytime heat events dominated in frequency and intensity, whereas humid night time events have become more dominant over the last couple of decades. The higher frequency of night time events in the last two decades was punctuated by an unusually extreme heat wave in July 2006, which was the largest heat event on record since 1948 (Gershunov et al., 2009; Knowlton et al., 2009). Night time heat waves in 2001, 2003, and 2006 each set successive magnitude records, and although daytime heat wave activity over this period increasing significantly, most recent extreme daytime events were essentially daytime expressions of unprecedented night time events. Again in early September 2020, an intense heat wave set records in many locations in California, breaking all-time single day high temperatures across the San Francisco Bay Area and forcing the National Weather Service to issue heat alerts for nearly the entire state.

There have been several recent nationwide (United States) studies of human demographics associated with neighbourhood temperature differences experienced during heat waves in major U. S. cities. For instance, Reid et al. (2009) analyzed demographic variables associated with heat-related mortality in ten large U. S. cities and reported that education, poverty, race, and social isolation were the variables that explained the highest fractions of variance in intra-urban heat vulnerability. In studies covering most major U. S. cities, O'Neill et al. (2003), Medina-Ramon et al. (2006), and Reid et al. (2009) all reported that individuals with a high school education or less had higher heat-related mortality rates than did individuals with additional years of education. In a study of surface heating patterns across over 100 U. S. cities, Hoffman et al. (2020) suggested that in areas dominated by construction of large housing complexes and factories in the mid-1900s, currently home to populations of relatively low income and communities of colour, structures built of cinder block and brick will retain daytime heat, and maintain high temperatures throughout the night.

The influence of green vegetation on cooling of urban heat islands (UHI) has been well-documented in many review publications, including that by Hoffman et al. (2020), who reported that patterns of surface heating across 108 U. S. cities were partly attributable to the relative coverage of impervious (high-asphalt) surface cover versus vegetation canopy cover in these areas, and also in reviews from Bowler et al. (2010) and Susca et al. (2011). It is cited in most of these studies that vegetation canopies cool an area by direct shading of the ground surface and indirectly by the transpiration of water through leaves.

The influence of other land cover features on UHIs have been less well characterized – These features include parking lots, roadways, railways, dark rooftops, parcel and building areas and heights, water bodies, exposed ground and bare soil sometimes under construction. Along these lines, Scott et al. (1999) found that parking lot temperatures in California were warmer than irrigated turf nearby, and that even sparse tree canopy exerted a cooling effect on both parking lots and vehicle surface temperatures. Ronnen (2018) reported that higher rooftop albedos in Los Angeles were associated with reductions in neighbourhood-scale temperature.

The purpose of the present study was to better understand the geography and demographics of extreme urban heat events in Santa Clara County and the city of San Jose, California, also known as the home of Silicon Valley. Santa Clara is California's 6th largest county with a population of more than 1,781,000 (as of the 2010 census). San Jose, the 10th most populous city in the U. S., is California's third largest city and the most populous city in the San Francisco Bay Area. Santa Clara County is the economic center for high technology in the U. S. and has the third highest gross domestic product (GDP) per capita in the world (Trujillo and Parilla, 2016). Nevertheless, according to the U. S. Census Bureau's American Community Survey (2011-2015), 10% of the population of San Jose lived below the poverty line, a percentage that has been slightly lower than the national average of 13.1%. According to the Public Policy Institute of California, the poverty rate in Santa Clara County is currently around 15.5% and the top income families earn 16 times more than low income families in the County (Bohn et al., 2017).

This study first analyzed the influence of several urban cover features in the northern portion of Santa Clara County – streets/roadways, parcel sizes and densities, impervious surfaces, and irrigated shrub/lawn cover – on county-wide surface heat

patterns measured by the Landsat satellite sensor during early August 2020. In the second part of the study, social demographic and household population variables for Santa Clara County from the U. S. Census Bureau were correlated against satellite surface temperature (again in early August 2020) averaged by census tract to reveal potential associations of family structure, education levels, disabilities, and country of birth (U. S. versus foreign) with local neighborhood heat conditions.

2. Data and Methodology

2.1 Satellite Image Data

The thermal infrared sensor (TIRS) is an instrument on the Landsat 8 satellite that collects images within the thermal range (10–12.5 µm; USGS, 2018). Landsat 8 image data are retrieved every 16 days, with each scene being 170 km north–south by 183 km east–west. The TIRS has a pixel size of 100 m that was re-gridded to 30 m to match Landsat multi-spectral bands. Image data were gathered by the Landsat-8 sensor on 9 August 2020 at approximately 11:45 AM Pacific Time.

Land surface temperature (LST) from the Landsat TIRS bands was calculated to represent the temperature of the Earth's surface in Kelvin (K). The computational methods used to derive LST images were described by Cook et al. (2014) and included use of radiative transfer models, incorporation of sensor-relative spectral response, adjustments for surface emissivity, and conversion of surface radiance to temperature

Vegetation green cover was mapped of the study area from the Normalized Difference Vegetation Index (NDVI), derived from 30-m resolution Landsat imagery obtained on 9 August 2020. NDVI was computed from two Landsat surface reflectance bands using the equation:

(NIR – Red) / (NIR + Red)

where Red is the reflectance band from 0.63 to 0.69 µm, and NIR is the near-infrared reflectance band from 0.77 to 0.90 µm. The potential NDVI ratio of -1 to 1 was delimited to low values of NDVI (near zero) indicating barren ground cover and high NDVI values (above 0.5) indicating a predominate green vegetation cover in the pixel, typical of densely wooded rangelands, creek sides, parkways, or croplands (Lentile et al., 2006).

2.2 Streets and Parcel Data Layers

Polygon shapefiles for streets and land parcel layers were downloaded from the County of Santa Clara Open Data Portal at www.data.sccgov.org. The parcel lot layer is updated annually around August of each year, whereas the streets layer is updated quarterly.

2.3 Census Databases

The U. S. Census tract shapefile boundaries and data tables for Santa Clara County were downloaded for all available social and household demographic data from the American Community Survey webpage (U. S. Census Bureau, 2018). These county-level data profiles summarized the demographic variables for any selected geographic area, both in terms of total numbers and percentages by census tract.

2.4 Statistical Analysis

The Zonal Tabulation and Statistics Tools in ArcGIS Desktop version 10.7 (ESRI) were used to calculate area mean, standard deviations, and totals for digital polygons (or raster layers) within the zones defined by another polygon layer (e.g., temperature classes, census tracts). The internal conversion for an input polygon zone used the cell center method in the ArcGIS Polygon to Raster Tool to first rasterize the input using the pre-set raster cell size. Once an input polygon zone was converted using the same cell size and cell alignment of the base raster layer, statistics (e.g., Mean, Maximum, Minimum, and Standard Deviation) of cells values within each zone were computed by overlaying the zones on the rasterized layer. Standard errors (SE) of the mean LST classes and associated geographic variables were next computed, and a significant difference (at $p < 0.05$; 95% confidence level) was resolved wherever two mean values were separated by two SE of their respective mean values (McDonald, 2014).

Non-linear correlation analysis between LST and census demographic variables was carried out with second-order polynomial regression. In polynomial regression, different powers of the X variable (X, X^2, …) are used to test whether they increase the R^2 significantly over simple linear regression (McDonald, 2014). At a census tract sample number of greater than 215 for the county, any

Pearson's R^2 greater than 0.2 was considered significant at $p < 0.05$ (95% confidence level) for a two-tailed test (Kenney and Keeping, 1962). Therefore, any correlation coefficient greater than 0.2 was construed as a meaningful statistical association between LST and a given demographic variable over the entire county.

3. Results

3.1 Influence of urban cover features on LST

The geography of LST on 9 August 2020 for northern Santa Clara County was mapped in Figure 1 into polygon classes to show the mid-day surface heating patterns of all urbanized areas that were not dominated by continuous green vegetation cover (with NDVI > 0.5), as is indicative of dense wooded hillsides, creek sides, and parkways. The majority of the county fell into the LST class of $35 - 40^{\circ}$ C (Figure 2a), and the surrounding LST classes (lower and higher) were near normally distributed around that mean class range. The higher LST classes of > 45 °C were mapped largely in the eastern half of the county, whereas the lower LST classes of < 30 °C were mapped for water bodies, most of which were located on San Francisco Bay salt ponds north of San Jose.
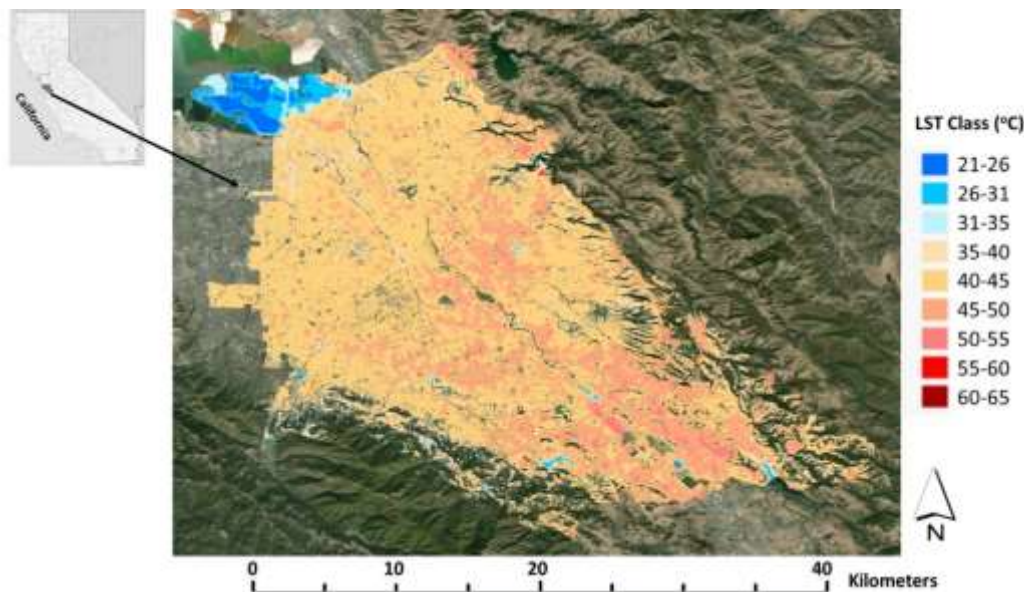

Figure 1: Map of land surface temperature (LST) classes for northern Santa Clara County from Landsat satellite imagery collected on 9 August 2020.

The distribution of all LST contiguous polygon areas shown in Figure 1 revealed that the highest fraction (40%) covered just a single Landsat pixel equivalent to 900 m^2, whereas another 20% of LST covered more than a hectare in area (Figure 2b). The LST class with the highest mean contiguous polygon area (at 23.6 ha) was measured with surface temperature between 45 – 50 °C.

The largest contiguous U. S. Census tracts of high LST > 45 °C were located in the following sections of the county: Alum Rock, Reid-Hillview Airport near E. Capitol Expressway, Cambrian Park south of Blossom Hill Road, and on either side of U. S. Highway 101 near Coyote Creek Park. Areas of the highest (> 50 °C) LST were mapped at locations where there were large fields of exposed ground and extensive impervious (high-asphalt) surfaces, such as parking lots and airport runways (photo examples in Figure 3, left panel). The U. S. Census tracts with largest contiguous areas of relatively low LST < 40 °C were located in the following sections of the county: Mission College and Great America Theme Park, Montague Expressway near River Oaks Park, Guadalupe River Park, and Willow Glen. Areas of relatively low (< 40 °C) LST were detected at locations where there was an abundance of small trees lining the streets and (irrigated) grass lawns on lots (photo examples in Figure 3, right panel).
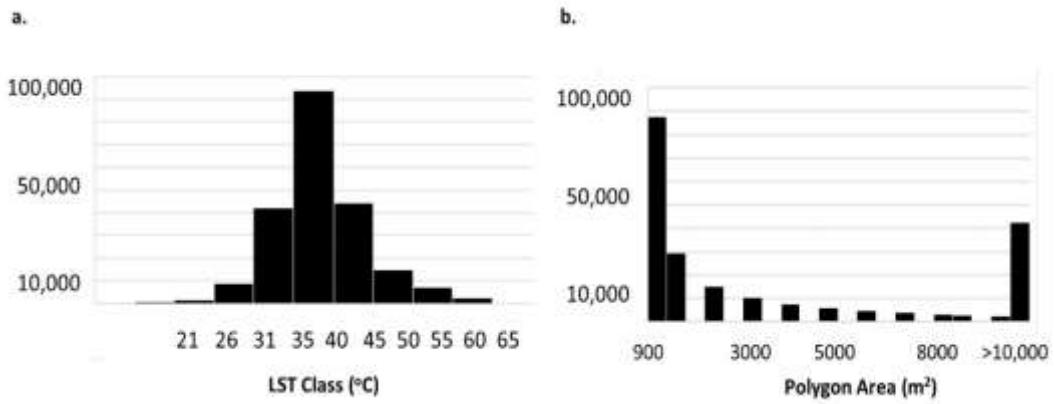
Eur. J. Clim. Ch. 2021, 3(2) 01-10

5

Figure 2: Histogram distribution plots of polygon counts for (a) LST classes and (b) LST polygon areas for northern Santa Clara County from Landsat satellite imagery collected on 9 August 2020.

Figure 3: Street-level photos of representative locations where relatively low (< 40 °C) LST (right panel) and high (> 50 °C) surface temperature (left panel) was mapped from Landsat satellite imagery collected in August 2020 (Locations shown in map Figure 5).

Developed urban areas with NDVI lower than 0.5 typically range from having a predominant coverage by an impervious surface (or bare ground) with a NDVI near 0.1, up to coverage by continuous green irrigated lawns, shrubs, and small trees at a NDVI level closer to 0.4. The change in mean NDVI with increasing LST class for the county showed that there was an exponential decrease from an NDVI level typically around 0.35 for LST areas mapped at between 35 – 40 °C, decreasing to NDVI levels at around 0.17 for LST areas mapped at > 55 °C (Figure 4a). The differences in mean NDVI levels for all LST classes less than 55 °C were significant at $p < 0.05$.
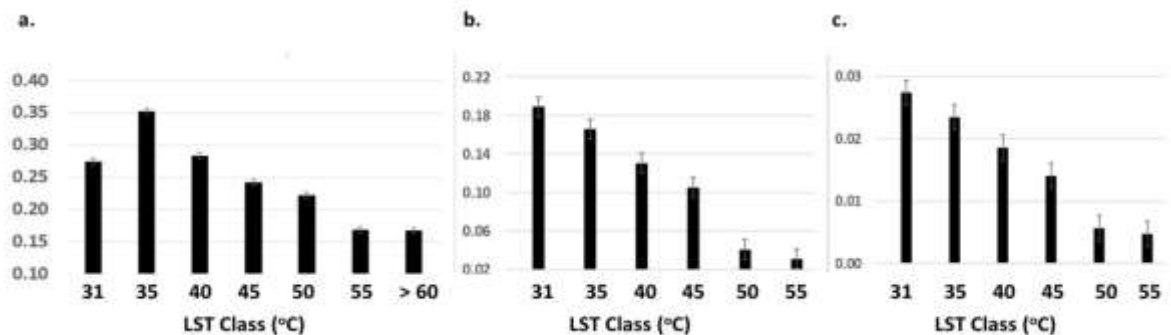

Figure 4: Plots of LST class averages for (a) NDVI per cent vegetation green cover, (b) per cent paved road area cover, and (c) per cent parcel boundary area cover for northern Santa Clara County from Landsat satellite imagery collected on 9 August 2020.
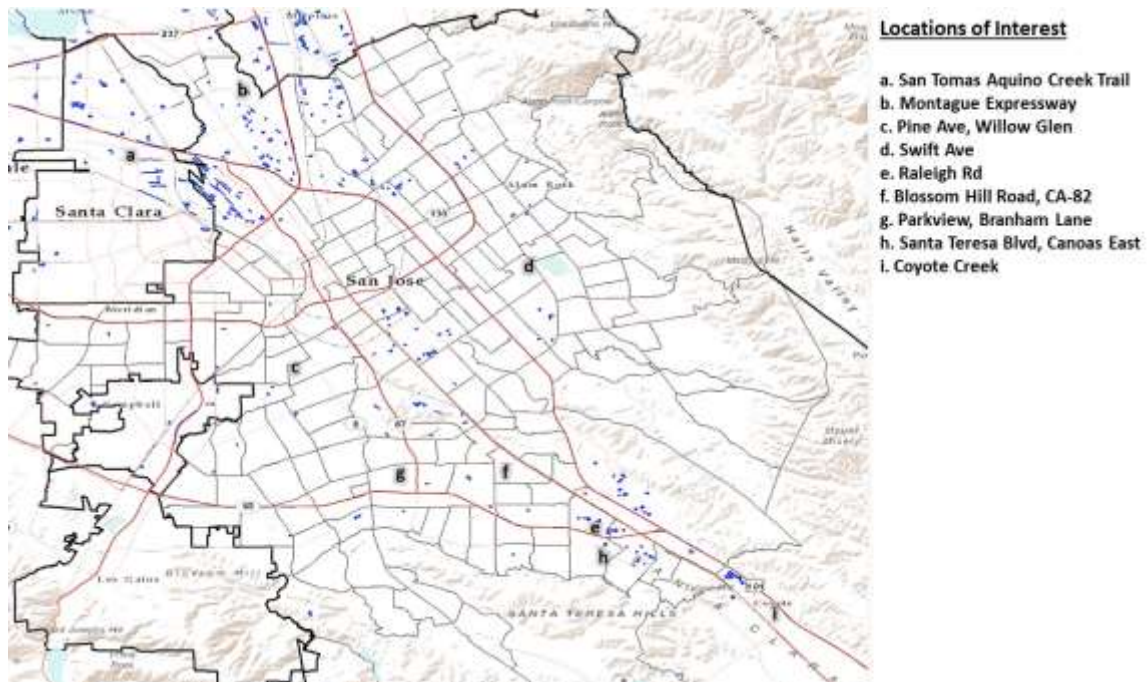

Figure 5: Map of the largest contiguous impervious surface features in Santa Clara County, outlined in blue polygon boundary lines.

To further evaluate the summer 2020 surface temperatures of the largest contiguous impervious surface features in Santa Clara County, 375 different parking lots, highways, airport runways, and building rooftops, covering an average area of 5186 m^2 (1.3 acres) were visually identified from Google Maps satellite imagery and delineated with polygon boundaries for statistical analysis (Figure 5). It was determined that the Landsat surface temperature on 9 August 2020 for these large impervious surface features ranged from 44.3

°C to 45.6 °C, with an overall mean of 45 °C and a standard deviation of around 0.5 °C.

The change in the mean percent cover of paved road surfaces with increasing LST class showed that there was a progressive decrease from road cover levels above 15% for cooler LST polygon areas mapped at between 30 – 40 °C, down to road cover percent at less than 10% for the warmest LST polygon areas mapped at > 50 °C (Figure 4b). The differences in mean percent cover of road surfaces among all the different LST classes below 50 °C were significant at $p < 0.05$.

The change in the mean percent cover of parcel boundaries with increasing LST class across the county showed that there was a steep decrease from parcel cover density typically above 1% for cooler LST polygon areas mapped at between 30 – 45 °C, down to parcel cover density at less than 1% for the warmest LST polygon areas mapped at > 50 °C (Figure 4c). The differences in mean percent cover of parcel boundary areas among all the different LST classes lower than 50 °C were significant at $p < 0.05$.

3.2 Associations of social and household demographics with summer LST

The correlations of social and household demographic data summaries for Santa Clara County from the American Community Survey (U. S. Census) tracts with average LST for each corresponding tract in early August 2020 showed that four demographic variables had significant ($p < 0.05$) $R^2 > 0.2$ correlation values, namely percent of female members in a household, average family size per household, percent of population with less than a 9th grade education, and percent of population with a college bachelor's degree education (Figure 6). These correlation results suggested that tracts with higher summer heat wave temperatures also had higher family sizes and more female members in the household. Similarly, tracts experiencing higher heat wave temperatures also had more household members with less than a high school education and fewer members with a college bachelor's degree.
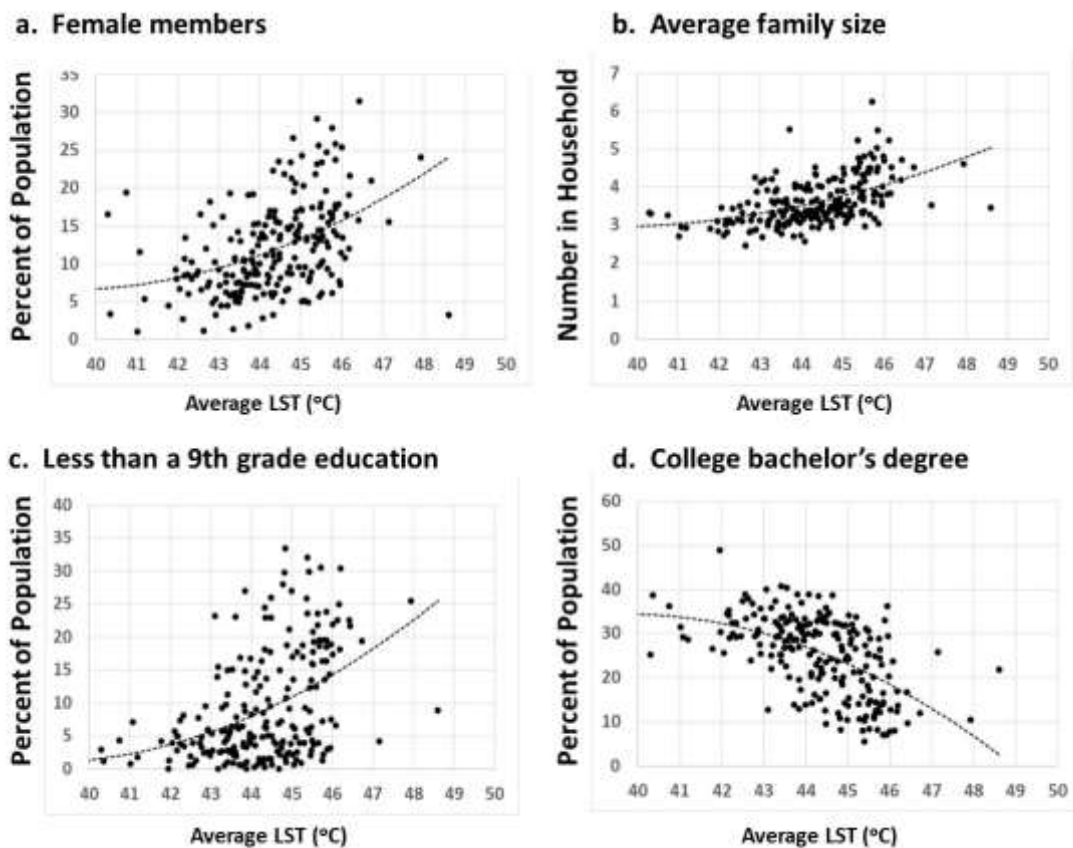

Figure 6: Correlation plots of LST averages (estimated for 9 August 2020) by U. S. Census tract versus (a) percent female members of the household, (b) average family size per household, (c) percent of population with less than a 9th grade education, and (d) percent of population with a college bachelor's degree education. Non-linear regression fits are shown as dashed lines. All four regression R^2 correlation values were greater than 0.2 ($p < 0.05$) for $N = 219$ census tracts.

The notable social demographic variables that were not found to be significantly correlated with average summer surface temperature for each corresponding census tract included: place of birth as native (born in United States) versus foreign born; marital status; households with one or more people 65 years and over; population with disabilities, number of grandparents, population 3 years and over enrolled in nursery school, elementary school, or high school.

4. Discussion

Among the most important findings of this study was that the surface temperature of the largest contiguous impervious surface features in Santa Clara County was significantly higher, at a mean value of 45 °C in early August 2020, than the majority of the other areas across the entire county that fell into a LST range of 35 – 40 °C. These several hundred large parking lots, runways, wide highways, and building rooftops, each covering an average of six Landsat pixels in surface area, varied only slightly in LST (± 0.5 °C) on that date. With minimal green vegetation cover on any of these impervious surfaces, they represent urban features that can disproportionately heat the surrounding neighborhoods (indicated in Figure 5) to elevated levels, and hence are prime candidates for mitigation with cooling management techniques such as solar energy panels and green rooftops. The results from this LST analysis further showed that tracts in Santa Clara County with even partial coverage by irrigated green lawns, shrubs, and small trees can still cool a tract effectively, presumably by absorbing sunlight before it reaches the darker ground and by moving water from the soil to the atmosphere through foliage.

The higher density of paved road surfaces that are common in densely populated residential and business areas surround more property lots with shaded rooftops and more irrigated green lawns with small trees, at least compared to large highway corridors. Major highways in the Bay Area have mostly bare ground between wide roadway surfaces. Tracts with relatively few roads but many large impervious surfaces, such as large (non-residential) retail shopping centers and malls with surface parking lots, consistently showed elevated LST compared to residential tracts with a higher density of road surfaces. Furthermore, in densely populated residential areas, smaller parcel lots close together can be seen to have more shaded rooftops and irrigated green lawns with small trees, compared to relatively large parcel lots that have shopping centers and business parks with more cement-covered impervious surfaces and less vegetation cover.

At the scale of the entire landscape surrounding Santa Clara County, the pattern of detecting higher LSTs largely in the eastern half of the county may be explained in part by the aspect of the hillslopes being more western- and southern-facing in the eastern half of the county. This aspect difference would expose more areas to direct sunlight on southern facing slopes for more hours of the day in the summer months in the warmest sections of the county, like the eastern side of U. S. Highway 101 near Coyote Creek Park and along Santa Teresa Blvd.

The association between heat waves and higher rates of mortality in the elderly and in lower-income groups has been well-documented in studies by Gronlund et al. (2014), Uejio et al. (2011), and Harlan et al. (2013). However, the present study of extreme urban heat patterns in Santa Clara County was not based on mortality rates. Rather, the question posed here was what are the associations of social and population demographics with local neighborhood heat conditions that can put residents at risk for heat-related health impacts? Along these lines, NPR (2019) reported on a study designed to the determine the link between heat and income levels in several U. S. cities and found that low-income neighborhoods are more likely to be hotter than their wealthier counterparts. However, few published studies for California urban centers have addressed questions like this and hence the results presented here are the first of their kind in many respects.

The finding that, in Santa Clara County, urban surface temperatures in early August were significantly correlated with average family size and male/female composition per census tract may indicate that the warmest neighborhoods, namely around Alum Rock Ave, Blossom Hill Road near CA-82, Parkview at Branham Lane, and along Santa Teresa Blvd (locations labelled in Figure 5), had a tendency toward higher numbers of female members of the household with larger than average family sizes. Most of the tracts in the county that showed average August surface temperatures above 46 °C were reported with average family sizes between 4 and 7 persons. This implies that a higher number of persons per household must endure heat waves living within the same dwelling in the hottest sections of San Jose and Santa Clara County.

The finding of urban tracts in Santa Clara County that experience higher heat wave impacts also tend to have more household members with less than a high school education and fewer members with a college bachelor's degree has been corroborated by several previous publications covering major U. S. cities (O'Neill et al., 2003; Medina-Ramon et al., 2006; Reid et al., 2009; Harlan et al, 2013).

Furthermore, Gronlund et al. (2014) asserted that differences in heat-associated health outcomes by educational completion levels are frequently mediated by a variety of related factors, such as income disparities, occupational opportunities, unemployment, or cognitive deficits, and that social programs and public health measures targeting these more proximate factors would likely be the most effective.

5. Conclusion

This study demonstrates that satellite thermal reflectance imagery for neighborhood- and parcel-scale investigations of UHI impacts has suitable spatial coverage at regular (bi-monthly) time intervals and is available at no cost to local governments. Nonetheless, more research is needed to better understand the many interacting processes underlying the spatial distribution of heat-vulnerable places and their relationships to human discomfort, displacement, illness, and death during extreme heat events. Questions that should be addressed further include: Do large impervious surfaces such as parking lots and dark (non-residential) rooftops contribute significantly to local or regional heating during cloudless summer days in northern California? Can even sparse coverage (less than 10% total area) by irrigated lawns and small trees significantly cool the warmest neighborhoods where green vegetation covers in presently relatively low? Can installation of rooftop green plant cover or solar panels result in lower surface temperatures on larger (neighborhood) scales?

Acknowledgement

References

Bohn, S., Danielson, C., Levin M., Mattingly, M., & Wimer, C. (2017). The California Poverty Measure, Stanford Center on Poverty and Inequality. 2 pp.

Borden, K.. and Cutter, S. (2008). Spatial patterns of natural hazards mortality in the United States. Int. J. Health Geogr. 7: 64.

Bowler, D. E., Buyung-Ali, L., Knight, T. M., & Pullin, A. S. (2010). Urban greening to cool towns and cities: A systematic review of the empirical evidence. Landscape Urban Plan. 97(3), 147–155.

Centers for Disease Control CDC (2006). Heat-related deaths - United States, 1999–2003. Morb Mortal Wkly Rep, 55: 796–798.

Cook, M., Schott, J. R., Mandel, J., & Raqueno, N. (2014). Development of an operational calibration methodology for the Landsat thermal data archive and initial testing of the atmospheric compensation component of a Land Surface Temperature (LST) product from the archive. Remote Sensing, 6(11): 11244-11266.

Gershunov, A., D., Cayan, D., & Iacobellis, S. (2009). The great 2006 heat wave over California and Nevada: Signal of an increasing trend, J. Clim., 22, 6181–6203

Gershunov, A. & Guirguis, K. (2012). California heat waves in the present and future, Geophys. Res. Lett, doi: 10.1029/2012GL05297.

Gronlund, C. J. (2014). Racial and socioeconomic disparities in heat-related health effects and their mechanisms: a review. Current Epidem. Reports, 1(3): 165-173.

Guirguis, K., Gershunov, A., Schwartz, R., & Bennett, S. (2011). Recent warm and cold daily winter temperature extremes in the Northern Hemisphere, Geophys. Res. Lett., 38, L17701, doi:10.1029/2011GL048762.

Habeeb, D., Vargo, J., & Stone, B. (2015). Rising heat wave trends in large US cities. Nat. Hazards, 76, 1651–1665.

Harlan, S., Declet-Barreto, J., Stefanov, W., & Petitti, D. (2013). Neighborhood effects on heat deaths: Social and environmental predictors of vulnerability in Maricopa County, Arizona, Environ Health Perspect. 121(2): 197–204.

Hoffman, J., Shandas, V., & Pendleton, N. (2020). The effects of historical housing policies on resident exposure to intra-urban heat: A study of 108 US urban areas, Climate, 8 (1): 12.

Kenney, J. F. & Keeping, E. S. (1962). Confidence Interval Charts, 11.5 in Mathematics of Statistics, 3rd ed. Princeton, NJ, Van Nostrand, pp. 167-169

Knowlton K., Rotkin-Ellman, M., King, G., Margolis, H., Smith, D., Solomon, G., Trent, R., & English, P. (2009). The 2006 California heat wave: impacts on hospitalizations and emergency department visits. Environ Health Perspect., 117: 61–67

Lentile, L., Holden, A., Smith, A., Falkowski, M., Hudak, A., Morgan, P., Lewis, S., Gessler, P., & Benson, N. (2006). Remote sensing techniques to assess active fire characteristics and post-fire effects. Intern. J. Wildland Fire, 15(3): 319–345.

McDonald, J. H. (2014). Handbook of Biological Statistics (3rd ed.). Sparky House Publishing, Baltimore, Maryland.

Medina-Ramon, M., Zanobetti, A., Cavanagh, D., & Schwartz, J. (2006). Extreme temperatures and mortality: assessing effect modification by personal characteristics and specific cause of death in a multi-city case-only analysis. Environ Health Perspect, 114: 1331–1336.

National Public Radio (NPS) (2019). Analysis of heat and income in U.S. cities, Available online at https://github.com/nprapps/heat-income

O'Neill, M., Zanobetti, A., & Schwartz, J. (2003). Modifiers of the temperature and mortality association in seven US cities. Am J Epidemiol, 157(12): 1074–1082.

Reid, C., O'Neill, M., Gronlund, C., Brines, S., Brown, D., DiezRoux, A., & Schwartz, J. (2009). Mapping community determinants of heat vulnerability. Environ Health Perspect, 117(11): 1730– 1736.

Ronnen, L., Ban-Weiss, G., Chen, S., Gilbert, H., Goudey, H., Ko, J., Li, Y., Mohegh, A., Rodriguez, A., Slack, J., Taha, H., Tang, T., & Zhang, J. (2018). Monitoring the Urban Heat Island Effect and the Efficacy of Future Countermeasures. California Energy Commission. Publication Number: CEC-500-2019-020.

Scott, K., Simpson, J., & McPherson, E. (1999). Effects of tree cover on parking lot microclimate and vehicle emissions, J. Arboriculture 25(3): 129-142.

Susca, T., Gaffin, S., & Dell'Osso, G. (2011). Positive effects of vegetation: Urban heat island and green roofs, Environ. Pollution, 159: 2119e2126.

Trujillo, J., & Parilla, J. (2016). Redefining Global Cities, A joint project of JP Morgan Chase and the Brookings Institution, Metropolitan Policy Program, Available online at: https://www.brookings.edu/wp-content/uploads/2016/09/metro_20160928_gcitypes.pdf

Uejio, C., Wilhelmi, O., Golden, J., Mills, D., Gulino, S., & Samenow, J. (2011). Intra-urban societal vulnerability to extreme heat: the role of heat exposure and the built environment, socioeconomics, and neighborhood stability. Health Place. 17(2): 498-507

U. S. Census Bureau (2018). ACS Information Guide, Selected Social Characteristics in The United States, p. 8, Accessed most recently in August 2020 from www.census.gov.

U. S. Geological Survey (USGS) (2018). Landsat Surface Temperature (ST) Product Guide, Version 2.0, LSDS-1330, Department of the Interior, Sioux Falls, South Dakota,32 pp.

Wong, K.V., Paddon, A., & Jimene, A. (2013). Review of world urban heat islands: Many linked to increased mortality. Energy Resour. Technol., 135: 022101.